Electronic structure of ordered and disordered Cu-Ag alloys

N. C. Bacalis
Theoretical and Physical Chemistry Institute, National Hellenic Research Foundation, Vas. Constantinou 48, GR-11635 Athens, Greece

G. F. Anagnostopoulos and N. I. Papanicolaou
Department of Physics, University of Ioannina, P.O. Box 1186, GR-45110 Ioannina, Greece

D. A. Papaconstantopoulos
Complex System Theory Branch, Naval Research Laboratory, Washington, D.C. 20375-5345

(Received 12 July 1996)

We present a study of the electronic structure of Cu-Ag alloys. This work includes total-energy evaluations, band structure, and density of states (DOS) determinations using the augmented-plane-wave method for the $L1_2$, $B1$, and $B2$ structures. We also study the corresponding disordered phases of these alloys by the tight-binding coherent potential approximation. Our results confirm the $B2$ and $L1_2$ (Cu reach) as the stable structures of these systems. We compare the DOS with experiment and other calculations, and confirm the absence of both magnetism and superconductivity in these alloys. Finally we estimate charge transfer for these alloys from Cu to Ag. [S0163-1829(96)08848-0]

I. INTRODUCTION

In the process of obtaining the phase diagram of Cu-Ag, Cu-Au, and Ag-Au alloys, Wei *et al.*[1] calculated by the linear-augmented-plane-wave method the band structure of the ordered A_nB_{4-n}, $(n=0, 1, 2, 3, 4)$ compounds. The results from ordered compounds were used in Ref. 1 via a three-dimensional Ising model, to obtain thermodynamic properties. Here we present in more detail the calculations of the band structure of Cu_3Ag and CuAg, using the semirelativistic (excluding spin-orbit coupling) augmented-plane-wave (APW) method. In addition we have used the tight-binding coherent-potential approximation (TB-CPA) in order to obtain the density of states (DOS) of the disordered alloys $Cu_{0.75}Ag_{0.25}$ and $Cu_{0.50}Ag_{0.50}$. We compare the DOS and other related properties with other calculations and experiment, when available. We have adjusted the APW muffin-tin sphere sizes in order to obtain charge transfers[2] consistent with CPA and experiment.

Cu_3Ag crystallizes in the $L1_2$ structure (fcc unit cell with Ag at the corners and Cu at the face centers). By total-energy minimization we determined the lattice constant to follow Vegard's rule closely. For CuAg we performed calculations in the CsCl and NaCl structures. It turned out that CuAg has lower total energy in the CsCl ($B2$) than in NaCl ($B1$). For the disordered alloys in the TB-CPA formalism, an energy shift is necessary for meaningful comparison with experiment. We have established a shift-determining procedure based on the d-band separation of the well-known Cu_3Au, which we consider as a prototype (see, for example, Refs. 2 and 3). For the ordered alloys, Wertheim, Mattheiss, and Buchanan[3] proposed a shift of the Fermi level E_F in order to agree with experiments. A similar procedure was followed here, arising again from the prototype Cu_3Au. For the CPA calculations we used lattice constants that obey Vegard's rule, although this underestimates both the experimental and the theoretical values;[4] for $Cu_{0.75}Au_{0.25}$ we performed a calculation with the experimental lattice constant (7.1 a.u. vs 7.07 a.u. from Vegard's rule), and found no appreciable difference.

We found that disordering decreases DOS at E_F, $N(E_F)$, contrary to Cu-Au alloys.[5]

A study of $Cu_{0.95}Ag_{0.05}$ by the Korringa-Kohn-Rostoker (KKR) cluster CPA method reveals essentially a Cu fcc DOS with a small Ag peak at 6.8 eV below E_F.[6] Another KKR-CPA study[7] for $Cu_{0.50}Ag_{0.50}$ shows a DOS at 2 eV below E_F, and a Ag component at 6 eV below E_F. We make comparisons with these available studies.

II. METHODOLOGY

The band structure of the ordered alloys was calculated with the APW method,[8] where the core levels are treated fully relativistically as atomic levels, and the outer 11 elec-

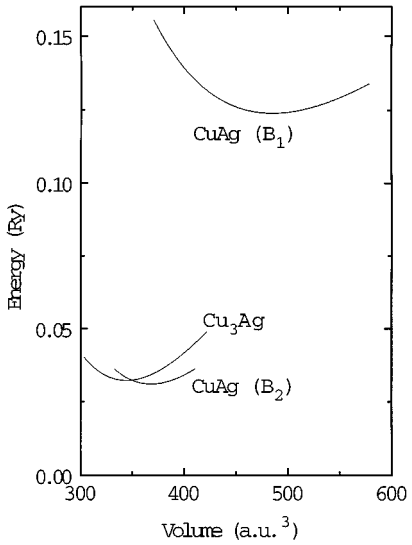

FIG. 1. The heat of mixing per atom as a function of the atomic volume for Cu-Ag alloys.

TABLE I. Equilibrium lattice parameters (bohr) and bulk moduli (Mbar).

Element/structure Compound		Lattice constant Expt.	Other calc.	Pres. calc.	Bulk modulus Expt.	Other calc.	Pres. calc.
Cu	fcc	6.83 [a]	6.673 [b]		1.31	1.424 [b]	
Ag	fcc	7.73 [a]	7.611 [b]		1.01	1.131 [b]	
CuAg	$B2$			5.688			1.499
CuAg	$B1$			9.900			0.879
Cu_3Ag	$L1_2$	7.10 [c]	7.05 [d]	7.008		1.37 [d]	1.581

[a]R.W.G Wyckoff, *Crystal Structures* (Interscience, New York, 1963), Vol. 1.
[b]Reference 16.
[c]Reference 7.
[d]Reference 1.

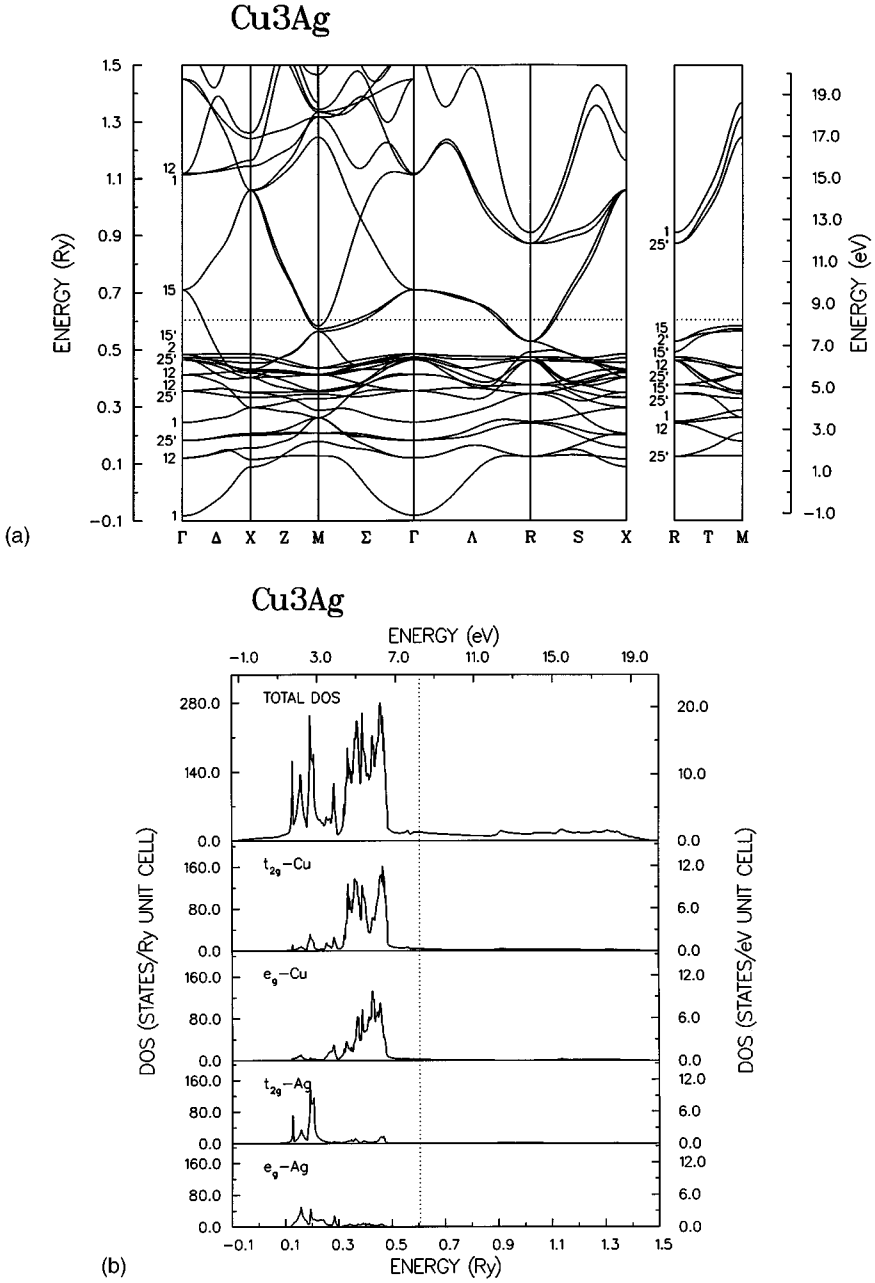

FIG. 2. (a) The band structure of ordered Cu_3Ag at the equilibrium lattice constant. (b) The total and the d-site-decomposed DOS.

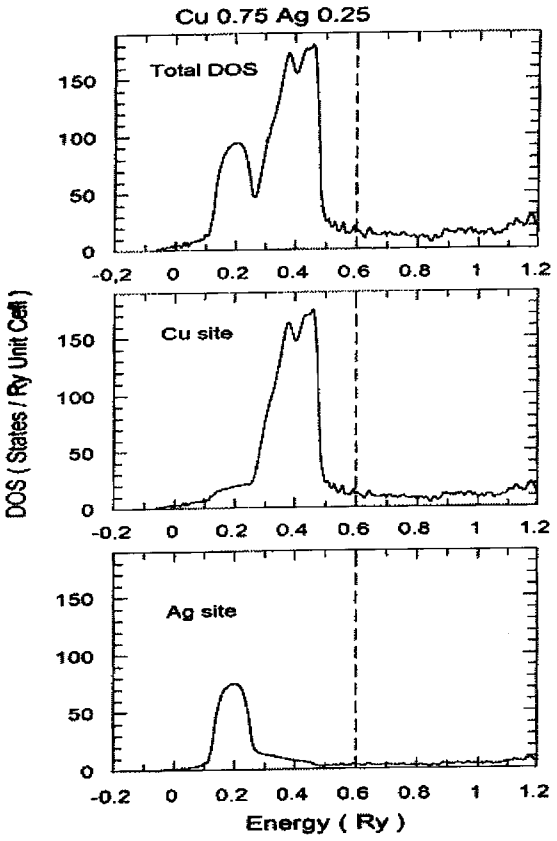

FIG. 3. Total, Cu-site, and Ag-site DOS's of $Cu_{0.75}Ag_{0.25}$.

trons of each element were treated as band electrons semirelativistically, i.e., by omitting spin-orbit coupling. The exchange and correlation was handled by the Hedin-Lundqvist[9] formalism. We used Janak's[10] expression for the total energy.

For the disordered alloys we used the TB-CPA treating diagonal disorder only.[11] The TB Hamiltonian matrix elements are treated as adjustable parameters, obtained by a two-center Slater-Koster (SK) fit[12] to the APW bands of the pure metals. Our SK parameters include first and second neighbors via the expression $p=ae^{-c^2R}$, where a and c are constants, different for each bond type $ss\sigma$, $pp\sigma$, $pp\pi$, etc. The off-diagonal parameters are geometrically averaged. The on-site parameters were shifted appropriately to account for the different energy scales of the individual components. An experimentation on our prototype Cu_3Au revealed that an appropriate on-site parameter shift would yield equal d-band separations in both the ordered and the disordered alloys.

III. RESULTS

In Table I we give the calculated lattice parameters and the corresponding bulk moduli for the ordered compounds and for reference the corresponding values for the pure elements. Our total energy results are given in Fig. 1, which shows the heat of mixing per atom, calculated by subtracting the percentage of the energy of fcc crystals Cu and Ag from the total energy of the alloy. In agreement with previous calculations,[1,6] the $L1_2$ and $B2$ structures are shown to be the stable structures for the corresponding Cu-Ag alloys.

A. Ordered Cu_3Ag

Previous studies[1,6] of Cu_3Ag address the issue of determining phase diagrams, but do not provide any details about the band structure *per se*, which would permit comparisons with our work. Our APW total-energy minimization yielded a $L1_2$ lattice constant of 7.008 a.u., in close agreement to other studies.[1,6] The band structure and the DOS are shown in Fig. 2. The d band extends from 7.1 to 1.6 eV below E_F, and consists of mainly two parts, the lowest Ag part between 7.1 and 4.1 eV, and the upper Cu part between 4.1 and 1.6 eV below E_F. Ag has some small-d component in the Cu part, extending up to 1.5 eV below E_F. The Cu d band remains essentially the same as in the pure fcc Cu, while the Ag d band develops some d interaction with Cu and narrows by approximately 1 eV upon alloying. The Ag t_{2g} and e_g components are reversed compared to the pure Ag fcc. The semirelativistic separation between the low-lying Ag t_{2g} and e_g peaks is 0.55 eV. The main interactions are Ag(e_g)-Cu(s) and Ag(t_{2g})-Cu(p), with a slight hybridization between Ag(e_g)-Cu(e_g)-Ag(s)-Cu(p), the Cu d states being essentially unmixed. In summary we can say that Ag loses its pure fcc character and it is influenced by its simple cubic environment; it interacts mainly with Cu s and p orbitals with a weaker d interaction between Cu and Ag. The Ag s states interact with Cu p states while hybridizing weakly with Ag e_g states.

B. Disordered $Cu_{0.75}Ag_{0.25}$

We calculated $Cu_{0.75}Ag_{0.25}$ in the fcc structure by using the TB-CPA and SK parameters of pure Cu fcc and Ag fcc.[12] We shifted the Cu on-site parameters by -0.08 Ry to match the Cu-Ag d-band separation in the ordered Cu_3Ag. The CPA DOS are given in Fig. 3. The whole valence band extends up to 9.5 eV below E_F, and consists of two parts, the Cu part between 1.3 and 4.3 eV below E_F and the Ag part between 4.3 and 6.8 eV below E_F. These features are maintained in the APW DOS of the ordered Cu_3Ag, calculated directly in the $L1_2$ structure, but the CPA DOS is smoother. Takano, Imai, and Fukuchi[13] calculated with the KKR cluster CPA method the DOS of $Cu_{0.95}Ag_{0.05}$. Compared to the DOS of this alloy we can see some similarities: the existence of the Cu and Ag parts 3.4 and 2.0 eV wide, respectively, with comparable Cu and Ag peak positions separated by 3.4 eV.

TABLE II. Densities of states at E_F (in states/Ry cell), Fermi velocity (in 10^8 cm/s), electron-phonon interaction η_{Cu} and η_{Ag} (in eV/A^2), and the Stoner criterion $I_FN(E_F)$.

Compound	$N(E_F)$	$N_{Cu}(E_F)$	$N_{Ag}(E_F)$	V_F	η_{Cu}	η_{Ag}	$I_FN(E_F)$
CuAg ($B2$)	7.94	4.37	3.57	1.29	0.217	0.303	0.0681
Cu_3Ag	17.67	14.00	3.67	1.46	0.371	0.151	0.0879

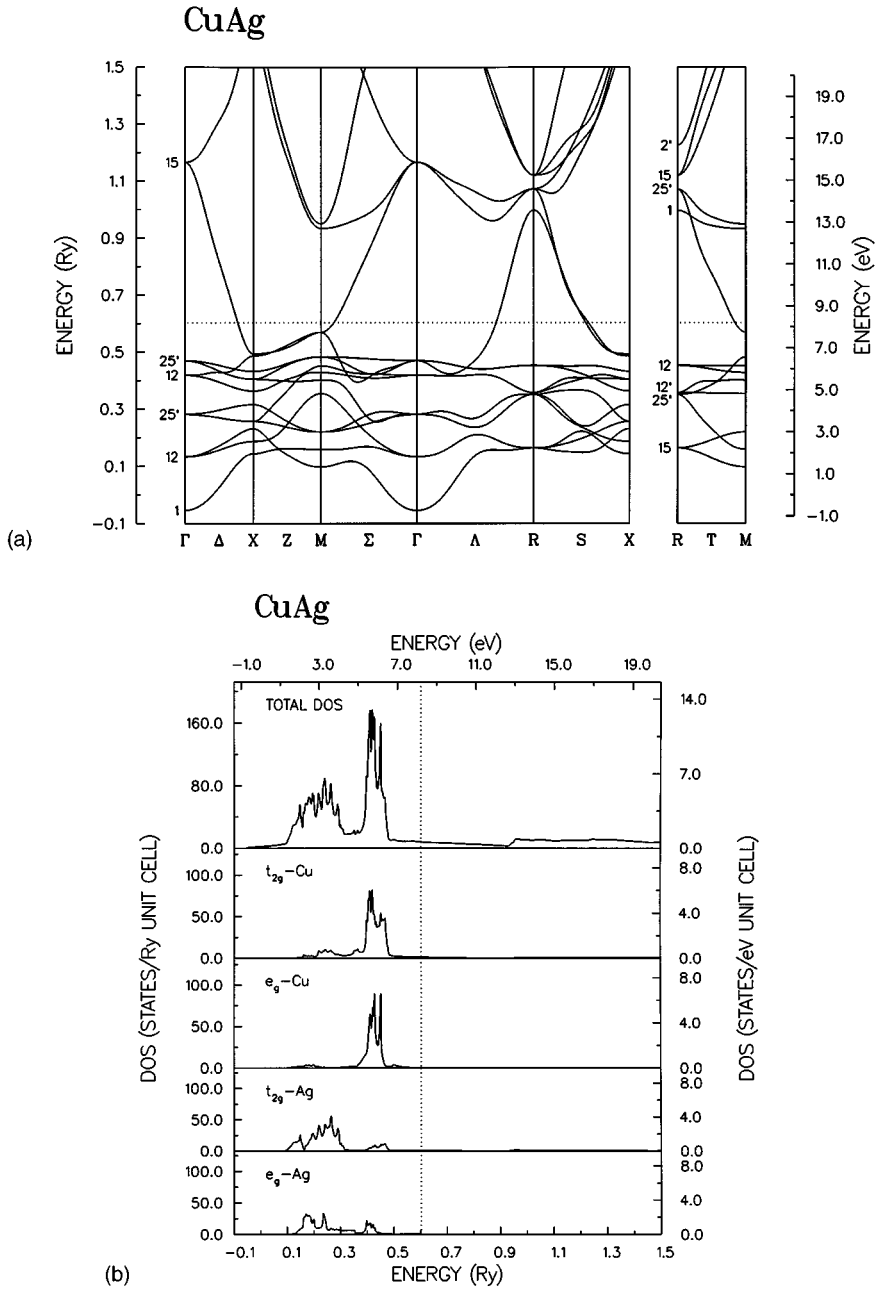

FIG. 4. (a) The band structure of ordered CuAg at the equilibrium lattice constant. (b) The total and the d-site-decomposed DOS.

C. Ordered CuAg

Since our calculations reveal that CuAg in the CsCl structure is more stable than NaCl, in Fig. 4 we present the band structure and DOS (total and angular momentum site-decomposed) in the CsCl structure. We see again the simple cubic symmetry characteristic that the lowest Ag t_{2g} and e_g components are reversed compared to the pure Ag fcc.[12] The DOS shows two rather separated parts, the lowest Ag part and the upper Cu part. The valence bands extend up to 9 eV below E_F. The Ag d part extends essentially between 6.8

TABLE III. Decomposed charges s, p, and d, and charge transfer.

Alloy	Cu					Ag				
	s	p	d	total	loss	s	p	d	total	gain
Pure metal (fcc)	0.74	0.35	9.91	11.00	0	0.65	0.35	10.01	11.00	0
Cu_3Ag	0.50	0.42	9.95	10.88	-0.12	0.60	0.59	10.17	11.36	0.36
$Cu_{0.75}Ag_{0.25}$	0.69	0.47	9.75	10.91	-0.09	0.73	0.66	9.88	11.27	0.27
CuAg	0.49	0.39	9.95	10.83	-0.17	0.57	0.51	10.09	11.17	0.17
$Cu_{0.50}Ag_{0.50}$	0.67	0.42	9.73	10.82	-0.18	0.72	0.59	9.87	11.18	0.18

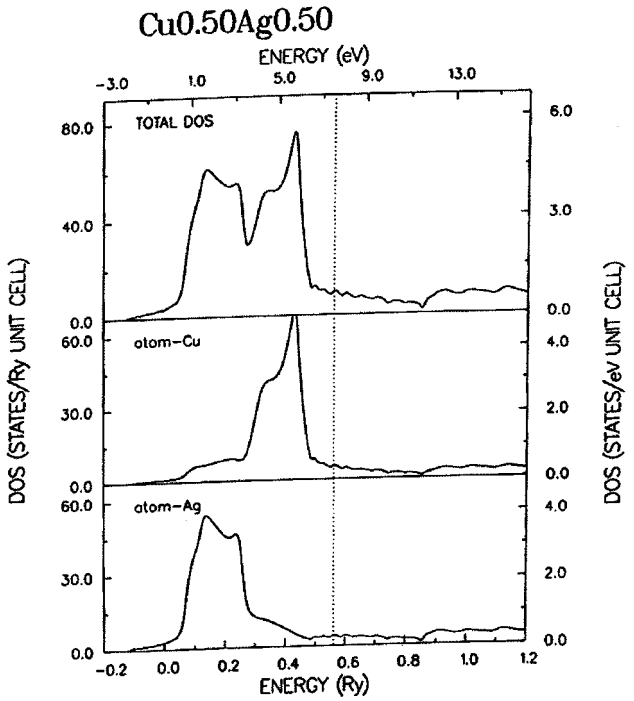

FIG. 5. Total, Cu-site, and Ag-site DOS's of $Cu_{0.50}Ag_{0.50}$.

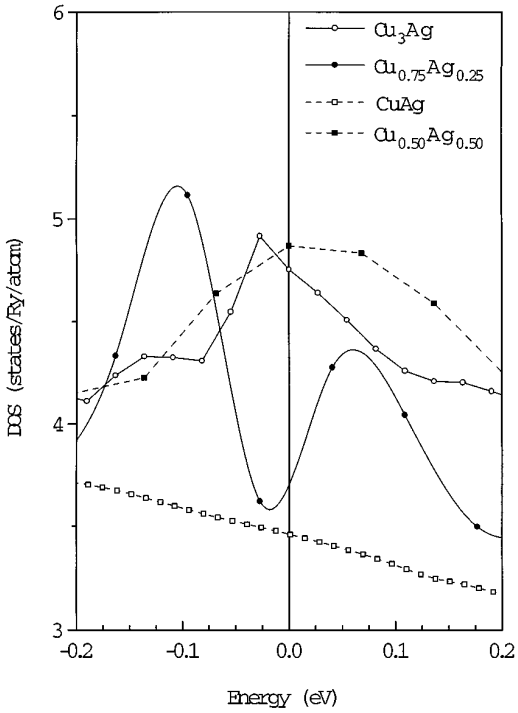

FIG. 6. The DOS around E_F for Cu-Ag alloys.

and 3.4 eV below E_F, but there is also some mixing with the Cu d part, which extends between 4 and 1.5 eV below E_F. The Cu e_g states do not hybridize appreciably with Ag d states, whereas the Cu t_{2g} states interact mainly with Ag t_{2g} states. Besides that, the Cu p states have some interaction with Ag e_g states, while some Ag s and p states interact slightly with Cu p and d states.

D. Disordered $Cu_{0.50}Ag_{0.50}$

We determined TB parameters corresponding to bcc Cu and Ag, and applied an energy shift in the CPA of -0.08 Ry as in $Cu_{0.75}Ag_{0.25}$. The resulting DOS is shown in Fig. 5 to consist of two broad features. The lower represents mainly Ag states located at about 6 eV below E_F, and the upper part represents Cu states centered at about 2 eV below E_F. The Cu peak is slightly narrower and higher than the Ag peak.

E. Densities of states at the Fermi level

The DOS at E_F, $N(E_F)$, is related to the specific-heat coefficient γ. For the Cu-Ag alloys it is shown in Fig. 6. We find a decrease of $N(E_F)$, and γ upon disordering for the 25% composition, but an increase for the 50% composition. In Table II we list the values of the total $N(E_F)$ as well as the components of the constituent atoms for the ordered compounds. If we account for the number of atoms in each unit cell, all of the ordered compounds have nearly the same $N(E_F)$. The Fermi velocity V_F, also listed in Table II, is 1.29×10^8 cm/s in CuAg and 1.46×10^8 cm/s in Cu_3Ag. These values of V_F are comparable to those of the pure elements.[12] In Table II we also give the electron-phonon interaction parameters η determined in the rigid muffin-tin approximation.[14] These values are similar to those of the pure elements, and much smaller than the values of η in typical superconducting materials, predicting no superconductivity. Finally, in Table II we list the Stoner criterion for magnetism $I_F N(E_F)$. These values are far from the value of 1.0 needed for the occurrence of magnetism, predicting paramagnetism.

F. Charge transfer

The APW analysis for the charge transfer depends on the size of the muffin-tin (MT) spheres. If equal MT spheres and an equipartition of the interstitial electrons are assumed, the results show the opposite direction of charge transfer than the CPA. On the other hand, if we use unequal MT spheres, which are proportional to the pure fcc elemental size, and if we partition the interstitial electrons proportionally to the volume of the unequal MT spheres, we find a charge transfer in very good agreement with our CPA results. In order to clarify this subject we performed similar APW and CPA calculations for the well-known Cu_3Au, and obtained the same trends concerning the charge transfer. Actually, the experiment shows[15] that in Cu_3Au upon alloying there is a charge transfer from Cu to Au consistent with electronegativity arguments. In addition, Kuhn and Sham[15] observed that the increase of the overall Au charge occurs in such a way so that the d charge decreases, while the s and p charges increase. We find that our CPA calculation, which does not suffer from the ambiguity of the choice of the relative size of the muffin-tin spheres, agrees well with experiment. Hence, unequal MT spheres, appropriately determined as above, are necessary to describe the correct charge transfer. It should be emphasized that the band structure, and DOS, have very weak dependences on the relative size of the MT spheres. In Table III we give the charge transfer with unequal MT spheres for the Cu-Ag alloys.

IV. SUMMARY

In summary, with the intent to complement previous studies, we presented comprehensive calculations of the electronic structure of Cu-Ag alloys equally balanced between total-energy results and band-structure analysis. Our study includes ordered and disordered phases of these compounds using the APW and CPA methods, respectively.

ACKNOWLEDGMENTS

This work was partially supported by NATO Grant No. CRG-940118 and by ΠΕΝΕΔ Grant No. 100/89 from the Greek Ministry of Energy and Technology. We thank Michael Mehl for many helpful discussions.

[1] S.H. Wei, A.A. Mbaye, L.G. Ferreira, and A. Zunger, Phys. Rev. B **36**, 4163 (1987).
[2] Z.W. Lu, S.-H. Wei, and A. Zunger, Phys. Rev. B **45**, 10 314 (1992).
[3] G.K. Wertheim, L.F. Mattheiss, and D.N.E. Buchanan, Phys. Rev. B **38**, 5988 (1988).
[4] P. Weinberger, V. Drchal, L. Szunyogh, J. Fritscher, and B.I. Bennett, Phys. Rev. B **49**, 13 366 (1994).
[5] K. Kokko, E. Ojala, and K. Mansikka, J. Phys. Condens. Matter **2**, 4587 (1990), and references therein.
[6] J.M. Sanchez, J.P. Stark, and V.L. Moruzzi, Phys. Rev. B **44**, 5411 (1991).
[7] J. Banhart, H. Ebert, R. Kuentzler, and J. Voitlander, Phys. Rev. B **46**, 9968 (1992).
[8] J.C. Slater, Phys. Rev. **51**, 846 (1937); L.F. Mattheiss, J.H. Wood, and A.C. Switendick, in *Methods in Computational Physics*, 8th ed., edited by B. Alder, S. Fernbach, and M. Rotenberg (Academic, New York, 1968).
[9] L. Hedin and B.I. Lundqvist, J. Phys. C **4**, 2064 (1971).
[10] J.F. Janak, Phys. Rev. B **9**, 3985 (1974).
[11] J.S. Faulkner, Prog. Mater. Sci. **27**, 1 (1982); P.M. Laufer and D.A. Papaconstantopoulos, Phys. Rev. B **35**, 9019 (1987).
[12] D.A. Papaconstantopoulos, *Handbook of the Band Structure of Elemental Solids* (Plenum, New York, 1986).
[13] N. Takano, S. Imai, and M. Fukuchi, J. Phys. Soc. Jpn. **60**, 1647 (1991).
[14] G.D. Gaspari and B.L. Gyorffy, Phys. Rev. Lett. **28**, 801 (1972).
[15] M. Kuhn and T.K. Sham, Phys. Rev. B **49**, 1647 (1994).
[16] M. Sigalas, D.A. Papaconstantopoulos, and N.C. Bacalis, Phys. Rev. B **45**, 5777 (1992).